Nanoscale

Accepted Manuscript

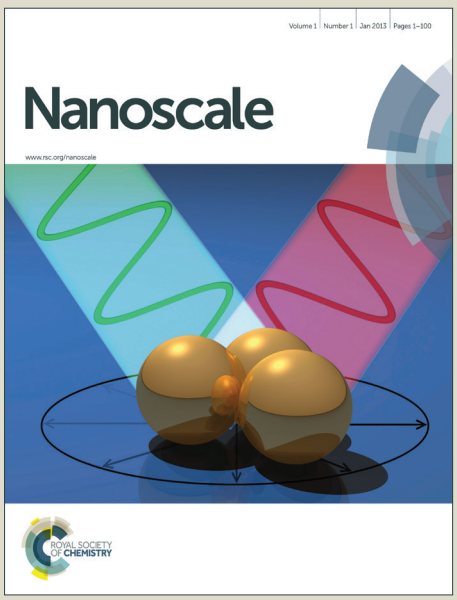

ROYAL SOCIETY OF CHEMISTRY

www.rsc.org/nanoscale

Nanopatterned Antimicrobial Enzymatic Surfaces Combining Biocidal and Fouling Release Properties

Qian Yu,[1] Linnea K. Ista,[4] and Gabriel P. López[1,2,3,4]*

[1]Department of Biomedical Engineering, [2]Department of Mechanical Engineering& Materials Science, and [3]NSF Research Triangle Materials Research Science & Engineering Center, Duke University, Durham, NC, 27708, USA.[4]Center for Biomedical Engineering , Department of Chemical and Nuclear Engineering, University of New Mexico, Albuquerque, NM, 87131, USA.

ABSTRACT

Surfaces incorporating the antimicrobial enzyme, lysozyme, have been previously demonstrated to effectively disrupt bacterial cellular envelopes. As with any surface active antimicrobial, however, lysozyme-expressing surfaces become limited in their utility by the accumulation of dead bacteria and debris. Surfaces modified with environmentally responsive polymers, on the other hand, have been shown to reversibly attach and release both live and dead bacterial cells. In this work, we combine the antimicrobial activity of lysozyme with the fouling release capability of the thermally responsive polymer, poly(*N*-isopropylacrylamide) (PNIPAAm), which has a lower critical solution temperature (LCST) in water at ~32°C. Nanopatterned PNIPAAm brushes were fabricated using interferometric lithography followed by surface-initiated polymerization. Lysozyme was then adsorbed into the polymer-free regions of the substrate between the brushes to achieve a hybrid surface with switchable antimicrobial activity and fouling-release ability in

response to change of temperature. The temperature triggered hydration and conformational change of the nanopatterned PNIPAAm brushes provides the ability to temporally regulate the spatial concealment and exposure of adsorbed lysozyme. The biocidal efficacy and release properties of the hybrid surface were tested against *Escherichia coli* K12 and *Staphylococcus epidermidis*. The hybrid surfaces facilitated the attachment of bacteria at 37°C for *E. coli* and 25°C for *S. epidermidis* and when the temperature is above the LCST, collapsed and dehydrated PNIPAAm chains expose lysozyme to kill attached bacteria. Changing temperature across the LCST of PNIPAAm (e.g. from 37°C to 25°C for *E. coli* or from 25°C to 37°C for *S. epidermidis*) to induce a hydration transition of PNIPAAm promoted the release of dead bacteria and debris from the surfaces upon mild shearing. These results suggest that nano-engineered surfaces can provide an effective way for actively mitigating short term bacterial biofouling.

1. Introduction

Bacterial contamination and the associated risk of infection are serious issues in a variety of arenas including water purification, public health, and the textile industry as well as in food packing and storage.[1-3] Therefore, endowing surfaces with antimicrobial properties to prevent biocontamination has been of great interest, in both medical and industrial settings.[4-6] Incorporation of biocidal agents on material surfaces is an effective means to kill or degrade attached bacteria and thus inhibit their proliferation and formation of biofilms.[7-9] Examples of synthetic biocides include polycations,[10-12] quaternary ammonium compounds,[13-14] and cationic conjugated polyelectrolytes.[15-16] However, such compounds may themselves have adverse health effects, both during their intended use and during their production. Enzymatic biocides which can exhibit a broad spectrum of antimicrobial activity, are environmentally friendly, require no toxic precursors or costly disposal protocols and offer sustainable production and are thus

attractive alternatives to synthetic antimicrobials.[17-18] The cell wall-degrading antimicrobial enzyme, lysozyme, is particularly attractive because its targets, the 1,4-beta-linkages between *N*-acetylmuramic acid and *N*-acetyl-D-glucosamine, are a fundamental feature of the bacterial cell envelope.[19] It is a robust enzyme, with surfaces retaining bacteriolytic activity under conditions likely to be encountered during sustained use.[20-24]

Although effective, surfaces that incorporate lysozyme suffer the same basic drawback as other biocidal surfaces: they can remain contaminated by dead bacteria and other debris, which not only results in a rapid reduction in biocidal activity, but also provides nutrients for other colonizers. Stimuli responsive polymers (SRPs) have been previously shown to controllably release adsorbed proteins,[25-27] attached mammalian cells,[28-30] and bacteria and biofilms.[31-34] The effectiveness of decontamination using a combination of antimicrobial activity and release with an incorporated SRP, has, however, proven to be highly dependent on the mode of action of the antimicrobial. An example is the integration of antimicrobial peptides (AMPs) into a thermo-responsive copolymer, resulted in effective killing, but also the continued attachment of dead bacteria to the surface after phase transition,[35] which is likely due to the insertion of the AMP molecules into the bacterial membranes. As a glycoside hydrolase, lysozyme is less likely to suffer from such limitations because it degrades the bacterial cellular envelope.

Recently, we developed a model multifunctional surface exhibiting the ability to control the attachment, killing and release of bacteria in response to temperature changes.[36] A biocidal, quaternary ammonium salt (QAS) was immobilized into polymer-free regions between nanopatterned, thermo-responsive poly(*N*-isopropylacrylamide) (PNIPAAm) brushes, which change their degree of solvation and modulate the spatial concealment and exposure of QAS, and thus biointerfacial interactions with bacteria, in response to temperature changes across the lower

critical solution temperature (LCST, ~32°C) of PNIPAAm in water. In this study, we extend our studies to incorporate lysozyme as an example of an environmentally benign, sustainable biocide. We show that the nanopatterned PNIPAAm/lysozyme hybrid surface facilitates the attachment of bacteria at temperatures either above or below the LCST of PNIPAAm at which bacterial attachment is favored for a particular organism (e.g. 37°C for *Escherichia coli* K12 or 25°C for *Staphylococcus epidermidis*).[31, 36] When the temperature is above the LCST, collapsed and dehydrated nanopatterned PNIPAAm chains expose lysozyme to kill attached bacteria. Changing temperature through the LCST (e.g. from 37°C to 25°C for *E. coli* or from 25°C to 37°C for *S. epidermidis*) to induce the hydration transition of PNIPAAm promotes the release of dead bacteria and debris from the surface.

2. Experimental section

2.1 Surface preparation

Preparation of self-assembled monolayers (SAMs) terminated with atom transfer radical polymerization (ATRP) initiators. Silicon wafers and cover slips were cleaned with "Piranha" solution (7:3(v/v) 98% H_2SO_4:30% H_2O_2; ***caution: piranha solution reacts violently with organic materials and should be handled carefully!***) to remove the organic residue. The wafers were subsequently rinsed with an abundance of ultrapure water and dried under a dry nitrogen stream. The cleaned samples were immersed in 10 mL of anhydrous toluene containing the ATRP initiator-terminated silane (2 vol.%) at room temperature for 24 h. These surfaces were rinsed thoroughly with toluene and dried under a nitrogen flow.

Photo-oxidation and patterning of SAMs. Interferometric lithography (IL) was performed using a two-beam interference system (Lloyd's mirror set-up) as reported previously.[37]

Nanopatterns of ATRP initiator were fabricated by exposing ATRP initiator immobilized SAMs to a diode-pumped, frequency-doubled neodymium-doped vanadate laser (Coherent, Verdi-V5) with a wavelength (λ) of 266 nm (energy dose of 13.9 J/cm^2).

Preparation of nanopatterned PNIPAAm/lysozyme hybrid surfaces. PNIPAAm polymer brushes were grafted from patterned SAMs of ATRP initiators using activators regenerated by electron transfer (ARGET)-ATRP.[37-39] Briefly, samples were immersed into a solution containing 14 mL methanol, 14 mL H_2O, 2.5 g NIPAAm, 3.15 mg $CuBr_2$, 34.5 mg ascorbic acid and 19.6 μL PMDETA for 6 min at room temperature. The samples were then removed from the solution, rinsed with an abundance of ultrapure water and methanol successively to remove both unreacted NIPAAm monomer and ungrafted PNIPAAm, and then dried under a nitrogen flow. As controls, PNIPAAm brushes were also grafted from unpatterned SAMs of ATRP initiators under identical polymerization conditions.

The nanopatterned PNIPAAm surfaces were first incubated in PBS at 37°C for 2 h and then transferred to a preequilibrated (37°C) lysozyme solution (5 mg/mL in PBS) for 2h to produce hybrid surfaces (referred to herein as "nanopatterned PNIPAAm/Lys" surfaces). The surfaces were then rinsed with an abundance of protein-free PBS and ultrapure water and dried under a nitrogen flow. Control surfaces were (i) degraded initiator SAMs (subjected to a blanket exposure by the laser beam (energy dose of 13.9 J/cm^2)) after adsorption of lysozyme as described above (referred to as "degraded initiator/Lys" surfaces), and (ii) nanopatterned PNIPAAm surfaces without adsorbed lysozyme. Each type of surface (test surface and controls) was prepared on both silicon wafers and glass coverslips.

2.2 Surface analysis

X-ray photoelectron spectroscopy. The elemental composition of surfaces was determined with a Kratos Analytical Axis Ultra X-ray photoelectron spectrometer (XPS) equipped with a monochromatic Al Kα source. High-resolution scans were acquired at a pass energy of 20 eV and a resolution of 0.1 eV. Survey scans were acquired with a pass energy of 160 eV and a resolution of 1.0 eV. All XPS data were analyzed using CASA XPS software. All binding energies were referenced to the main hydrocarbon peak designated as 285.0eV. Peak resolution was performed using a linear peak base and symmetric 30/70 Gaussian–Lorentzian component peaks.

Atomic force microscopy. Tapping-mode topographical measurements of nanopatterned PNIPAAm surfaces in air before and after adsorption of lysozyme were obtained with a Digital Instruments Dimension 3100 atomic force microscope (AFM). The corresponding section analysis (line profiling) was performed using Nanoscope Analysis software.

Contact angle goniometry. Contact angles were measured by a Rame-Hart model 100-00 contact angle goniometer either in air at 25°C using sessile drop method or in water using the captive bubble method at 25°C and 45°C. The temperature was controlled by a surrounding water jacket. Contact angle values reported are the average of six replicates.

***Ellipsometry*.** The thickness of unpatterned PNIPAAm brushes was measured with an M-88 spectroscopic ellipsometer (J. A. Woollam Co., Inc.). The thickness values reported are the average of three replicates. Ellipsometric data were fitted to obtain thicknesses of the polymer films using a Cauchy layer model with fixed A_n (1.47) and B_n (0.01) values.[40]

2.3 FITC-lysozyme adsorption. FITC-lysozyme was dissolved in PBS (pH 7.4) at a concentration of 1 mg/mL. Before protein adsorption, the samples were incubated in PBS at

25°C or 37°C for 2 h and then transferred to a preequilibrated (25°C or 37°C) FITC-lysozyme solution for 2h under static conditions. Following adsorption, the surfaces were immediately immersed in fresh, protein-free PBS for 5 min (three times) to remove loosely adsorbed protein. The surfaces were then briefly rinsed with ultrapure water to remove salt and dried under a nitrogen stream.

The adsorption of FITC-lysozyme was evaluated using a fluorescence microscope (Zeiss Axioimager) with a 40X objective. All images used for comparison of fluorescence intensities were obtained using identical exposure times, image contrast, and brightness settings. Fluorescence intensity of images was analyzed using Zeiss Axio Vision software. For each sample, 10 images from random areas across the sample surface were captured and analyzed to obtain average fluorescent intensity.

2.4 Attachment and detachment of bacteria. Attachment and detachment of bacteria on the sample surfaces were assessed using either an *E. coli* suspension (1×10^8 cells/mL in 0.85% NaCl) or an *S. epidermidis* suspension (3×10^7cells/mL in PBS).[31, 33] Briefly, prior to introduction of the sample surfaces, the cell suspensions were pre-equilibrated at 37°C (*E. coli*) or 25°C (*S. epidermidis*) in glass Petri dishes. The sample surfaces were placed on the bottom of a glass Petri dish, test surface up, and incubated in these suspensions at 37°C (*E. coli*) or 25°C (*S. epidermidis*) for 2 h unstirred. They were then rinsed gently with ultrapure water pre-equilibrated at 37°C (*E. coli*) or 25°C (*S. epidermidis*) to remove loosely attached cells and salts, and dried under a low-pressure stream of dry nitrogen. For bacterial detachment, the sample surfaces were washed under shear (estimated shear rate = 0.04 Pa) with 60 mL of 0.85% NaCl in water at 25°C (*E. coli*) or PBS at 37°C (*S. epidermidis*) delivered from a syringe, then rinsed in ultrapure water, and dried. The attached bacteria were examined using a phase contrast optical microscope (Zeiss

Axioimager) through a 40X objective and images of 15 randomly chosen fields of view were captured. For each sample, three replicates were performed and the density of adherent bacteria was analyzed by ImageJ (National Institutes of Health) to obtain the average and standard deviation.

2.5 Live/Dead assays. A standard live/dead staining assay was performed using the BacLight kit (Invitrogen, Grand Island, NY) to examine the biocidal activity of sample surfaces. Upon completion of the experimental treatments described above, the sample surfaces were immersed into a staining solution containing 1:1 mixture of SYTO 9 (3.34 mM) and propidium iodide (20 mM).[41] After incubation for 15 min in the dark, the surfaces were rinsed with ultrapure water and examined by fluorescence microscopy through a 40X air objective and images of 15 randomly chosen fields of view were captured. For each sample, three replicates were performed and the relative number of live (green) *vs.* dead (red) bacteria was analyzed by ImageJ to obtain the average and standard deviation.

2.6 Scanning electron microscopy. To observe the morphology of attached bacteria, the sample surfaces were rinsed gently in ultrapure water to remove the unattached cells, fixed in 2.5% glutaraldehyde solution for 2 h, dehydrated in a series of ethanol solutions (30-100%), and air-dried.[42] Before characterization, the samples were sputter coated with a 5 nm layer of gold. The surfaces were then examined using an FEI XL30 scanning electron microscope (SEM) at an accelerating voltage of 7 kV.

3. Results and discussion

3.1. Preparation and characterization of nanopatterned PNIPAAm/Lys hybrid surfaces

Nanopatterned PNIPAAm/Lys hybrid surfaces were prepared as illustrated in **Scheme 1**. First, we prepared a SAM of initiator terminated alkyl siloxanes, which was regio-selectively photodegraded at the nanoscale using UV-IL. We then used surface initiated ARGET-ATRP to graft PNIPAAm as we reported previously.[37] IL is a facile and inexpensive technique to provide periodic, nanoscopic patterns over relatively large surface areas (e.g. ~cm^2 for bacterial adhesion studies).[43] Finally, we incubated the resultant nanopatterned PNIPAAm surfaces in lysozyme solution (5 mg/mL in PBS) at 37°C for 2 h. Based on our previous studies,[37] we hypothesized that most lysozyme molecules adsorb into the polymer-free intervals between PNIPAAm brushes because at this temperature, the dehydrated PNIPAAm brushes adopt collapsed conformation to expose the unpatterned protein-adhesive substrate.

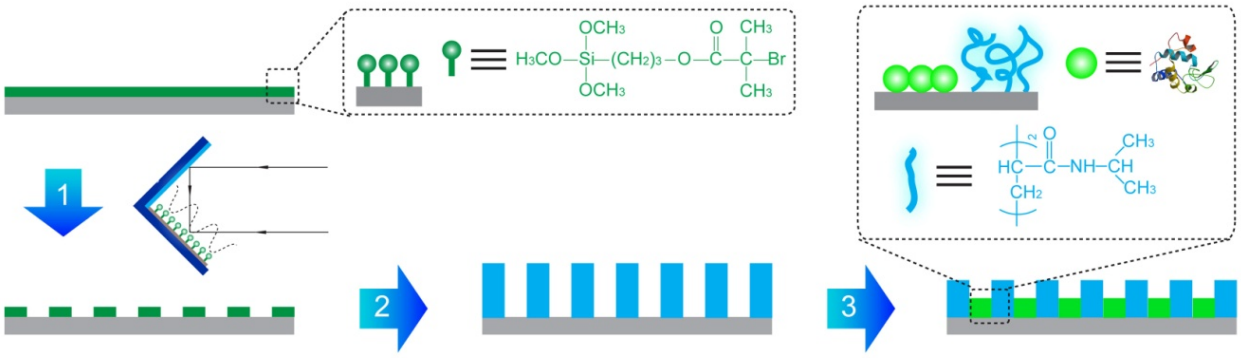

Scheme 1. Schematic depicting the procedure for preparation of nanopatterned PNIPAAm/Lys surfaces. Step1: IL patterning of SAM of ATRP initiators; Step 2: ARGET-ATRP of NIPAAm from pre-patterned initiator SAM; Step 3: Adsorption of lysozyme into the intervals between nanopatterned PNIPAAm lines at 37°C.

To confirm that lysozyme was binding to only the degraded initiator and not the PNIPAAm, we prepared a divided sample containing an area of degraded initiator and an area of unpatterned PNIPAAm (see **ESI**, **Scheme S1**) and incubated it in lysozyme solution under conditions identical to those for the patterned surfaces. After exposure to lysozyme, the degraded initiator portion showed an increased water contact angle (from 33±3° to 53±2°, **Fig. 1a**) and an increase in layer thickness (from 0.6±0.1 nm to 3.0±0.4 nm, **Fig. 1b**). Furthermore, within the XPS spectrum, the appearance of a nitrogen peak indicated the increased presence of adsorbed protein (**Fig. 1c,** and **ESI, Table S1**). In contrast, no such changes were observed on the part of the sample containing grafted PNIPAAm. Preferential absorbance of lysozyme onto the degraded initiator was further verified by fluorescence microscopic examination of FITC-lysozyme (**Fig. 1d**), in agreement with previous studies with other proteins.[37, 44] Additionally, AFM examination of nanopatterned PNIPAAm surfaces (period=455±27 nm) before and after adsorption of lysozyme revealed that the peak-to-valley value, as determined from line profile analyses of AFM images, decreased from 19.5±0.5 nm to 15.3±1.0 nm (**Fig. 2a,b**). The integration of lysozyme, however, did not influence the wettability of nanopatterned PNIPAAm surface; the resultant hybrid surface retained the same thermo-responsive wettability as the untreated nanopatterned PNIPAAm surfaces (**ESI, Fig. S1**). Taken together, these results strongly suggest that adsorption of lysozyme is restricted primarily to the nanopatterned regions of degraded initiator between the PNIPAAm brushes. We also measured the fluorescence intensity of nanopatterned PNIPAAm surfaces after adsorption of FITC-lysozyme below and above the LCST of PNIPAAm, and found ~1.7 fold increase in fluorescence intensity as incubation temperature increased from 25°C to 37°C. By comparison, there were no significant differences

in fluorescence intensity measured for either the degraded initiator surfaces and unpatterned PNIPAAm surfaces after adsorption of FITC-lysozyme at these two temperatures (**ESI, Fig. S2**). This thermo-responsivity of protein adsorption on the nanopatterned PNIPAAm surface is consistent with our previous report.[37]

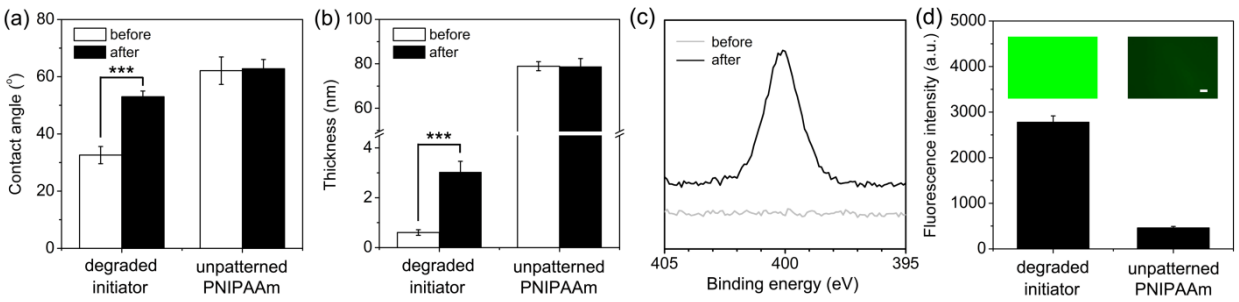

Fig. 1 (a) Water contact angle at 25°C and (b) layer thickness of degraded initiator and unpatterned PNIPAAm before and after adsorption of lysozyme (5 mg/mL in PBS) at 37°C for 2 h. (c) XPS high-resolution N_{1s} spectra of degraded initiator before and after adsorption of lysozyme (5 mg/mL in PBS) at 37°C for 2 h. (d) Adsorption of FITC-lysozyme (1 mg/mL in PBS) on the degraded initiator surface and unpatterned PNIPAAm surface at 37°C for 2 h. Representative fluorescence images are shown as insets. The scale bar in the images is equivalent to 20μm. In each case, data consist of the mean ± standard error (n=6; *** $p<0.001$)

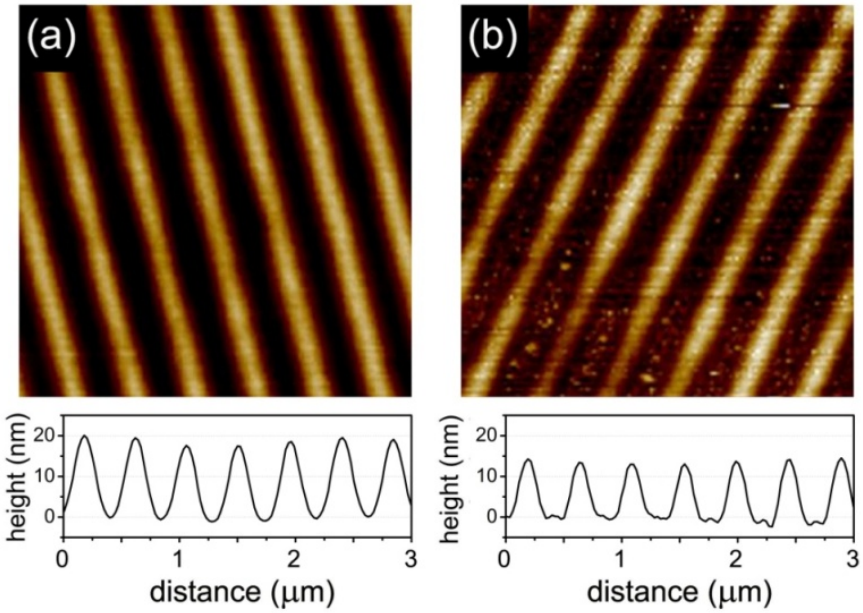

Fig. 2 Tapping mode AFM height images obtained in air of (a) a nanopatterned PNIPAAm surface and (b) a nanopatterned PNIPAAm/Lys surface; representative cross sections (line profiles) are shown beneath for each image. The size of images is 3×3 μm.

3.2. Biocidal activity of nanopatterned PNIPAAm/Lys surfaces

We tested the bactericidal activity of nanopatterned PNIPAAm/Lys hybrid surfaces against the Gram-negative bacterium, *E. coli,* and the Gram-positive bacterium, *S. epidermidis*. We also examined the degraded initiator/Lys surface and nanopatterned PNIPAAm surface as controls. We incubated samples either in an *E. coli* suspension (1×10^8 cells/mL) at 37°C for 2 h or in an *S. epidermidis* suspension (3×10^7 cells/mL) at 25°C for 2 h, then at 37°C for 1 h. The difference in incubation temperatures reflected the optimal temperatures, and thus, wettability at which *E. coli* and *S. epidermidis* have previously been shown to attach to PNIPAAm.[31, 33] We determined the viability of attached bacteria by a standard live/dead staining assay.[41] Most bacteria attached to the degraded initiator/Lys surfaces and the nanopatterned PNIPAAm/Lys surfaces fluoresced red,

indicating cell death (**Fig. 3a,b** and **d,e**); in contrast a majority of bacteria attached to the nanopatterned PNIPAAm and unpatterned PNIPAAm surfaces were alive (stained green, **Fig. 3c** and **f, ESI, Fig. 3a**). Moreover, as shown in SEM images, the bacteria attached to the nanopatterned PNIPAAm surfaces showed morphology characteristic of that of healthy bacteria (**Fig. 4c** and **f**). However, the bacteria attached to the degraded initiator/Lys surfaces and the nanopatterned PNIPAAm/Lys surfaces were morphologically less well defined, with considerable debris, indicating damage to their cellular envelopes (**Fig. 4a,b** and **d,e**), consistent with the known biocidal activity of lysozyme.[22, 45] The killing efficiency (defined as the ratio of dead bacteria and total bacteria) of nanopatterned PNIPAAm/Lys surfaces tested against *E. coli* and *S. epidermidis* was 61.3±6.1% and 76.4±8.6%, respectively, indicating higher antimicrobial efficacy of lysozyme against Gram-positive bacteria rather than Gram-negative bacteria, a result that may be due to the difference in the structure of their cell walls.[23]

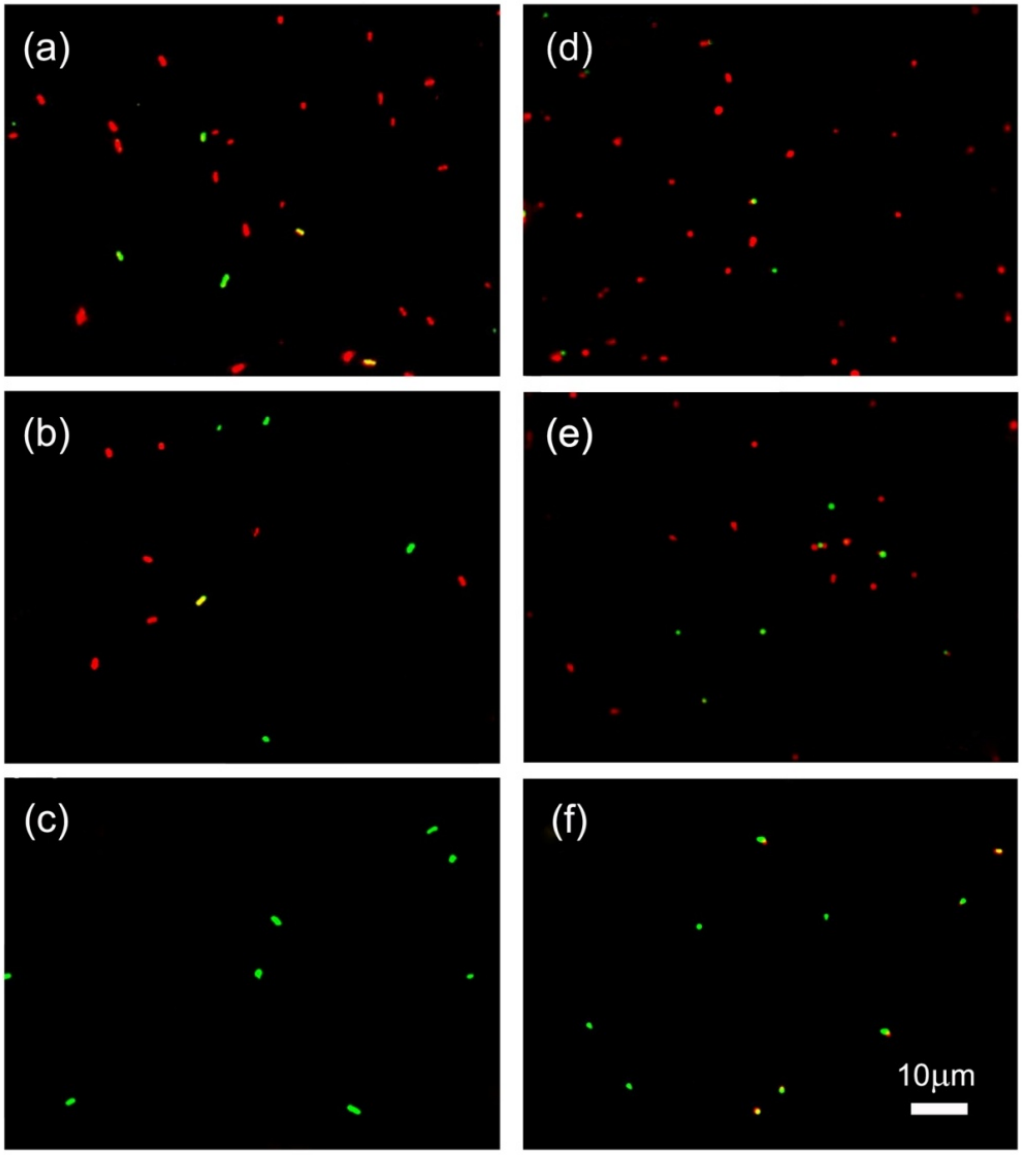

Fig. 3 Fluorescence microscopy images of attached bacteria. (a-c) *E. coli* and (d-f) *S. epidermidis*) exposed to live/dead stains (see text for details) on degraded initiator/Lys surfaces (a,d), nanopatterned PNIPAAm/Lys surfaces (b,e), and nanopatterned PNIPAAm surfaces (c,f). Surfaces were exposed to suspensions of *E. coli* at 37°C for 2 h or *S. epidermidis* at 25°C for 2 h then at 37°C for 1 h. Green staining indicates live bacteria, and red staining indicates dead bacteria.

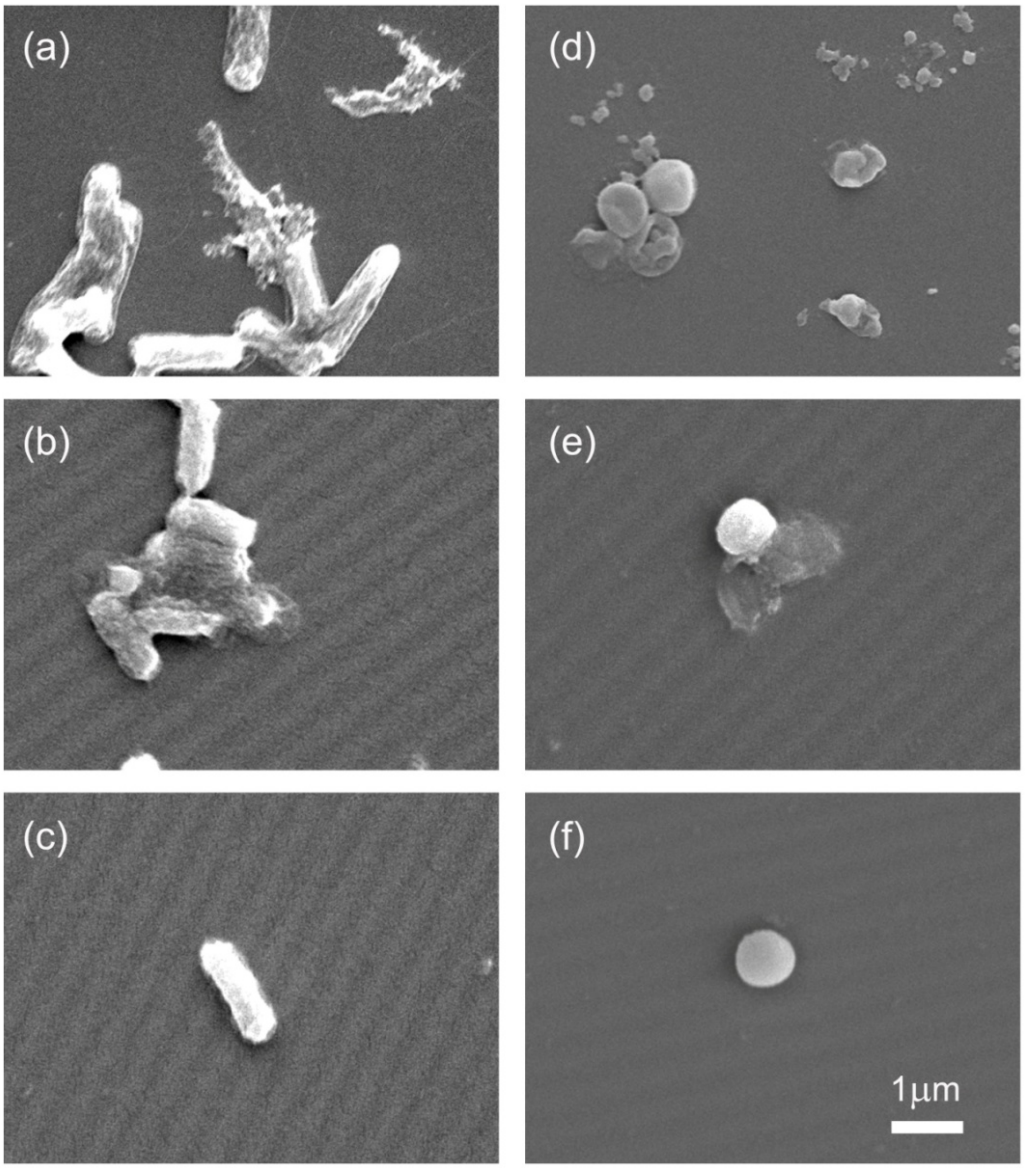

Fig. 4 SEM images of attached bacteria. (a-c) *E. coli* and (d-f) *S. epidermidis* on degraded initiator/Lys surfaces (a,d), nanopatterned PNIPAAm/Lys surfaces (b,e), and nanopatterned PNIPAAm surfaces (c,f). Surfaces were exposed to suspensions of *E. coli* at 37°C for 2 h or *S. epidermidis* at 25°C for 2 h then at 37°C for 1 h.

Next, we examined the effect of temperature on killing efficiency of the various surfaces, which were incubated in suspensions of *E. coli* or *S. epidermidis* at 37°C or 25°C for 2 h (**Fig. 5a, b**). The nanopatterned PNIPAAm/Lys surfaces exhibited significantly higher killing efficiency at 37°C than at 25°C (61.3±6.1% *vs.* 7.7±4.0% for *E. coli* and 76.4±8.6% *vs.* 23.4±8.0% for *S. epidermidis*). In contrast, for the control surfaces (degraded initiator/Lys and unpatterned PNIPAAm), the killing efficiency was similar at 37°C and 25°C, suggesting that the lysozyme activity is not affected by the difference in temperature. We thus propose a model to help interpret these differences in biocidal action as shown in **Scheme 2**. At 37°C, we believe the collapsed dehydrated PNIPAAm chains expose the adsorbed lysozyme so that it can contact and kill the attached bacteria; while at 25°C, the hydrated PNIPAAm chains cover the adsorbed lysozyme to block the access of attached bacteria. The thermally responsive conformation changes of PNIPAAm leads to the different killing efficiency, a result that is similar to our previous findings using synthetic biocides.[36]

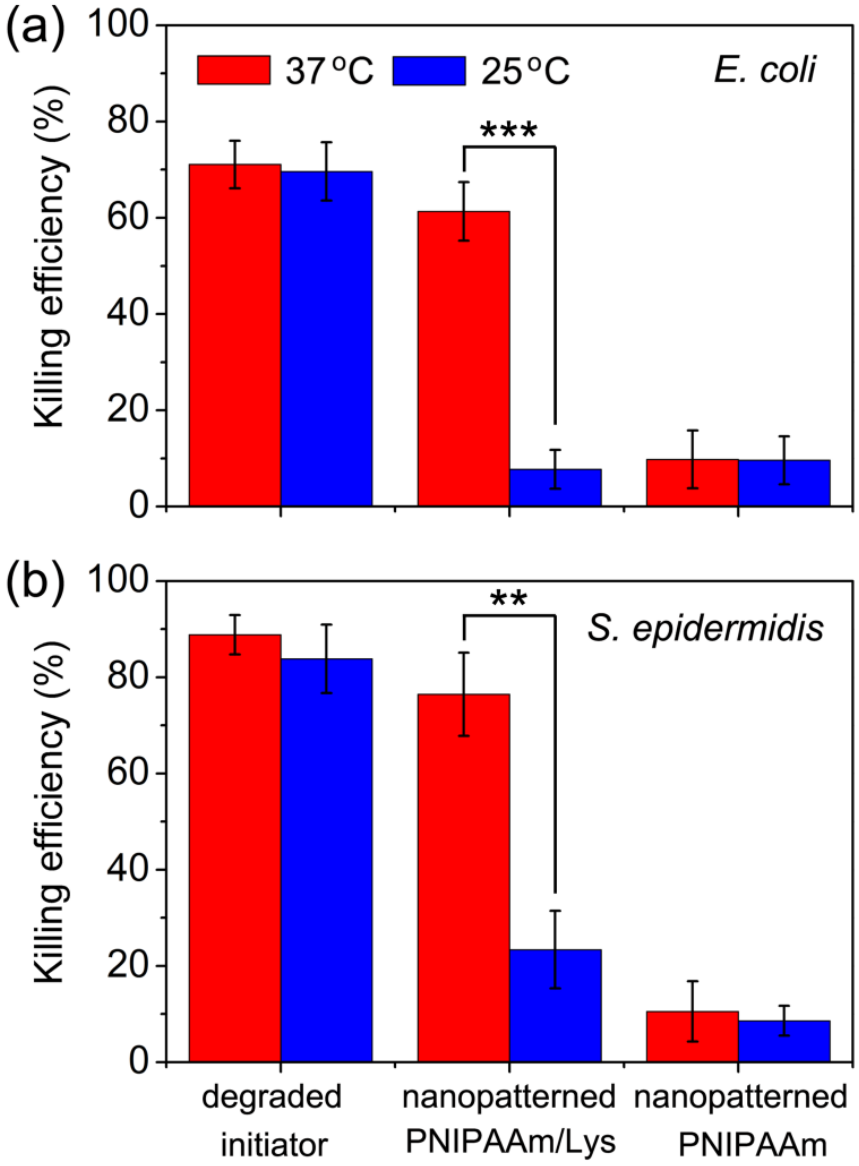

Fig. 5 Killing efficiency of surfaces against (a) *E. coli* and (b) *S. epidermidis* at different temperatures. The surfaces were incubated in suspensions of *E. coli* and *S. epidermidis* at 37°C or 25°C for 2 h. The killing efficiency was defined as the ratio of amount of dead bacteria and amount of total bacteria attached on these three surfaces at 37°C and 25°C. Error bars represent the standard deviation of the mean (n=3, ** P<0.01, *** P<0.001).

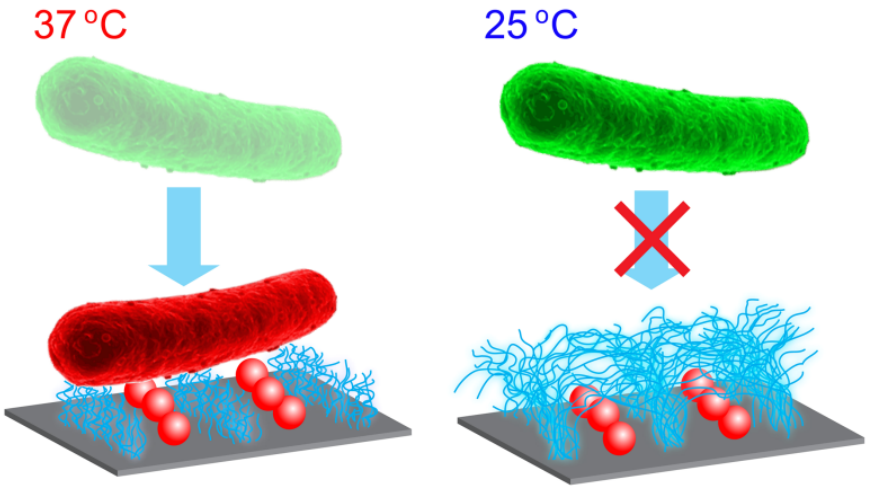

Scheme 2. Schematic illustration of interactions between bacteria (*E. coli*) and nanopatterned PNIPAAm/Lys surface at different temperatures.

3.4. Attachment and release of bacteria on nanopatterned PNIPAAm/Lys surfaces

A key feature of the nanopatterned PNIPAAm/Lys surfaces is their ability not only to attach and kill bacteria, but to release the dead cells and debris. To test the bacterial release capability, we first incubated the surfaces in suspension of bacteria at either 37°C (for *E. coli*) or 25°C (for *S. epidermidis*) for 2 h for attachment, and then rinsed the surfaces with either 0.85% NaCl in water at 25°C (for *E. coli*) or PBS at 37°C (for *S. epidermidis*). **Fig. 6** and **Fig. S3b** summarizes the number of bacteria attached initially and after transition through the LCST of PNIPAAm. The degraded initiator/Lys surfaces showed limited capability to release bacteria (the release ratio is lower than 40%), while other surfaces containing PNIPAAm released more than 70% of attached bacteria after rinsing. As controls, these surfaces were rinsed with the same buffer at 37°C (for *E. coli*) or 25°C (for *S. epidermidis*) in a similar manner and they showed less than 30% bacterial

detachment, consistent with our previous work with unpatterned PNIPAAm modified surfaces.[31, 33] This temperature-triggered fouling-release is due to the transition of surface hydration from a bacteria-attractive state to a bacteria-repellent state.[31-33, 36] Compared with nanopatterned PNIPAAm surfaces, nanopatterned PNIPAAm/Lys surfaces exhibited slightly larger bacterial attachment but a comparable release ratio. Taking the results together, we conclude that the hybrid surface combines the functional features of lysozyme (biocidal activity) and PNIPAAm (fouling-release ability) together into one system. By simply adjusting the temperature across the LCST, the hybrid surface switches its function to kill bacteria and to release bacteria.

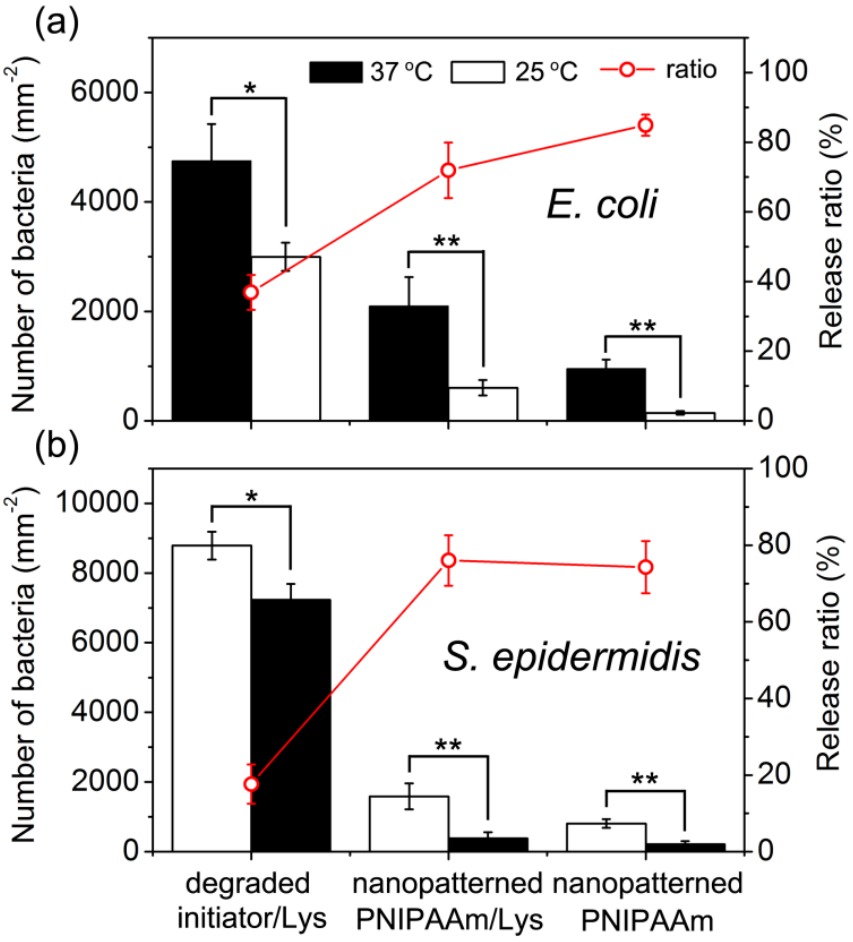

Fig. 6 Attachment and detachment of (a) *E. coli* and (b) *S. epidermidis* on different surfaces. The surfaces were incubated in suspensions of *E. coli* at 37°C or *S. epidermidis* at 25°C for 2 h and the average number of attached cells was determined. Then the surfaces were rinsed with 0.85% NaCl in water at 25°C (*E. coli*) or PBS at 37°C (*S. epidermidis*) and the remaining cells were counted. The bacterial release ratio is also shown. Error bars represent the standard deviation of the mean (n=3, * P<0.05; ** P<0.01).

We also used *E. coli* to examine the bactericidal and release properties of nanopatterned PNIPAAm/Lys hybrid surfaces upon repeated attachment and release cycles (**Fig. 7**). After two cycles of attachment and release, the surface exhibited slightly decreased release ratio but considerably reduced killing efficiency. The degraded biocidal activity might result from (i) the loss of physisorbed lysozyme during the cycling experiments and/or (ii) unavoidable contamination from the unreleased bacteria and debris (**ESI, Fig. S4**). In future studies, we will conduct a thorough investigation of a range of nanopattern parameters (e.g. nanopattern type, period, polymerization time) and enzyme binding methods (physisorption vs. chemisorption) to optimize the killing efficiency, the release efficiency and the reusability of the hybrid surfaces.

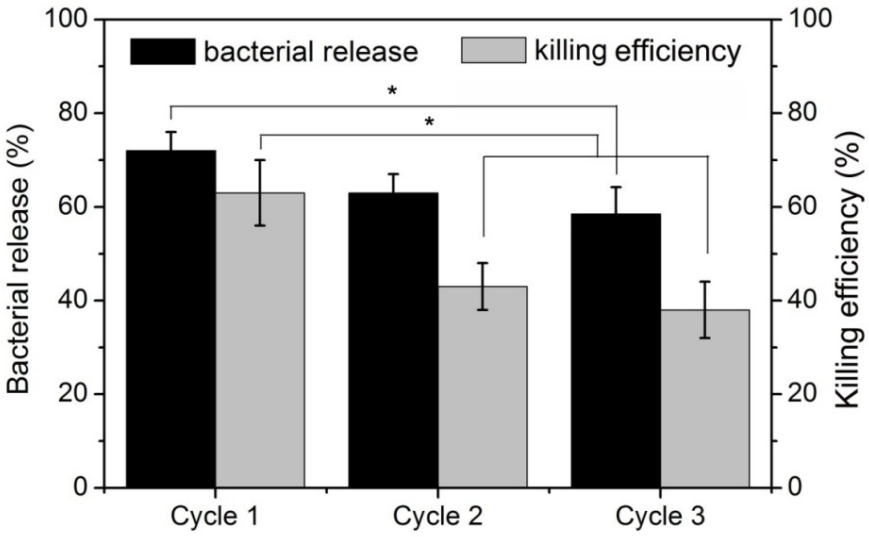

Fig. 7 Comparison of killing efficiency and bacterial release ratio of nanopatterned PNIPAAm/lysozyme hybrid surfaces after three cycles (attach-kill-release). Error bars represent the standard deviation of the mean (n=3, *p<0.05)

4. CONCLUSION

We have developed a hybrid surface which can attach, kill and release bacteria in a controllable manner by integration of lysozyme into thermally responsive nanopatterned PNIPAAm surfaces. We demonstrated that most lysozyme was adsorbed to the nanoscopic polymer-free regions of the substrate between PNIPAAm brushes. This system exploits the temperature dependent conformational changes of PNIPAAm in water to control the display of adsorbed lysozyme and thus switch the surface bioactivity. The nanopatterned PNIPAAm/Lys hybrid surface exhibited biocidal activity against attached bacteria when the temperature was above the LCST, while simultaneously allowing the easy removal of dead bacteria and debris by changing the temperature through the LCST of PNIPAAm (e.g. from 37°C to 25°C for *E. coli* or from 25°C to 37°C for *S. epidermidis*) to induce the transition of the hydration state of PNIPAAm brushes. These results provide a new strategy to engineer dual functional surfaces with both antimicrobial activity and fouling-release capability, which will be potentially useful for biomedical and industrial applications.

Electronic supplementary information (ESI). Materials and bacterial strains; preparation of macroscopically patterned surfaces; XPS and contact angle measurements; lysozyme adsorption at different temperatures; attachment, killing and release of bacteria on unpatterned PNIPAAm surfaces; and SEM study of sequential biocidal activity and fouling-release.

Corresponding Author

* Email: gabriel.lopez@duke.edu.

Acknowledgments

We are grateful for funding provided for support of this work from the Defense Threat Reduction Agency (Grant No. HDTRA1-11-1-0004), the Office of Naval Research (Grant No. N00014-10-1-0907) and the NSF's Research Triangle MRSEC (Grant No. DMR-1121107).

References

1 L. Hall-Stoodley, J. W. Costerton and P. Stoodley, *Nat. Rev. Microbiol.,* 2004, **2**, 95-108.

2 D. Pavithra and M. Doble, *Biomed. Mater.,* 2008, **3**, 1-13.

3 H. H. Tuson and D. B. Weibel, *Soft Matter,* 2013, **9**, 4368.

4 I. Banerjee, R. C. Pangule and R. S. Kane, *Adv. Mater.,* 2011, **23**, 690-718.

5 M. Charnley, M. Textor and C. Acikgoz, *React. Funct. Polym.,* 2011, **71**, 329-334.

6 K. G. Neoh and E. T. Kang, *ACS Appl. Mater. Interfaces,* 2011, **3**, 2808-2819.

7 J. A. Lichter, K. J. Van Vliet and M. F. Rubner, *Macromolecules,* 2009, **42**, 8573-8586.

8 L. Timofeeva and N. Kleshcheva, *Appl. Microbiol. Biotechnol.,* 2011, **89**, 475-492.

9 A. Muñoz-Bonilla and M. Fernández-García, *Prog. Polym. Sci.,* 2012, **37**, 281-339.

10 J. C. Tiller, C. J. Liao, K. Lewis and A. M. Klibanov, *Proc. Natl. Acad. Sci. U S A,* 2001, **98**, 5981-5985.

11 S. B. Lee, R. R. Koepsel, S. W. Morley, K. Matyjaszewski, Y. J. Sun and A. J. Russell, *Biomacromolecules,* 2004, **5**, 877-882.

12 H. Wang, L. Wang, P. Zhang, L. Yuan, Q. Yu and H. Chen, *Colloids Surf., B,* 2011, **83**, 355-359.

13 B. Gottenbos, H. C. van der Mei, F. Klatter, P. Nieuwenhuis and H. J. Busscher, *Biomaterials,* 2002, **23**, 1417-1423.

14 J. Song, H. Kong and J. Jang, *Colloids Surf., B,* 2011, **82**, 651-656.

15 L. K. Ista, D. Dascier, E. Ji, A. Parthasarathy, T. S. Corbitt, K. S. Schanze and D. G. Whitten, *ACS Appl. Mater. Interfaces,* 2011, **3**, 2932-2937.

16 H. Chong, C. Nie, C. Zhu, Q. Yang, L. Liu, F. Lv and S. Wang, *Langmuir,* 2012, **28**, 2091-2098.

17 S. A. Onaizi and S. S. J. Leong, *Biotech. Adv.,* 2011, **29**, 67-74.

18 B. Thallinger, E. N. Prasetyo, G. S. Nyanhongo and G. M. Guebitz, *Biotechnol. J.,* 2013, **8**, 97-109.

19 K. Glinel, P. Thebault, V. Humblot, C. M. Pradier and T. Jouenne, *Acta Biomater.,* 2012, **8**, 1670-1684.

20 S. Amiri, R. Ramezani and M. Aminlari, *J. Food Prot.,* 2008, **71**, 411-415.

21 S. I. Park, M. A. Daeschel and Y. Zhao, *J. Food Sci.,* 2004, **69**, M215-M221.

22 Q. Wang, X. Fan, Y. Hu, J. Yuan, L. Cui and P. Wang, *Bioprocess Biosyst. Eng.,* 2009, **32**, 633-639.

23 S. Yuan, D. Wan, B. Liang, S. O. Pehkonen, Y. P. Ting, K. G. Neoh and E. T. Kang, *Langmuir,* 2011, **27**, 2761-2774.

24 A. Caro, V. Humblot, C. Méthivier, M. Minier, M. l. Salmain and C.-M. Pradier, *J. Phys. Chem. B,* 2009, **113**, 2101-2109.

25 Q. Yu, H. Chen, Y. Zhang, L. Yuan, T. Zhao, X. Li and H. Wang, *Langmuir,* 2010, **26**, 17812-17815.

26 D. L. Huber, R. P. Manginell, M. A. Samara, B.-I. Kim and B. C. Bunker, *Science,* 2003, **301**, 352-354.

27 Q. Yu, Y. Zhang, H. Chen, Z. Wu, H. Huang and C. Cheng, *Colloids Surf., B,* 2010, **76**, 468-474.

28 M. A. Cooperstein and H. E. Canavan, *Langmuir,* 2010, **26**, 7695–7707.

29 A. Kikuchi and T. Okano, *J. Control. Release,* 2005, **101**, 69-84.

30 D. B. Liu, Y. Y. Xie, H. W. Shao and X. Y. Jiang, *Angew. Chem. Int. Ed.,* 2009, **48**, 4406-4408.

31 L. K. Ista, S. Mendez and G. P. Lopez, *Biofouling,* 2010, **26**, 111-118.

32 L. K. Ista, S. Mendez, V. H. Perez-Luna and G. P. Lopez, *Langmuir,* 2001, **17**, 2552-2555.

33 L. K. Ista, V. H. Perez-Luna and G. P. Lopez, *Appl. Environ. Microbiol.,* 1999, **65**, 1603-1609.

34 D. Cunliffe, C. D. Alarcon, V. Peters, J. R. Smith and C. Alexander, *Langmuir,* 2003, **19**, 2888-2899.

35 X. Laloyaux, E. Fautré, T. Blin, V. Purohit, J. Leprince, T. Jouenne, A. M. Jonas and K. Glinel, *Adv. Mater.,* 2010, **22**, 5024-5028.

36 Q. Yu, J. Cho, P. Shivapooja, L. K. Ista and G. P. Lopez, *ACS Appl. Mater. Interfaces,* 2013, **5**, 9295-9304.

37 Q. Yu, P. Shivapooja, L. M. Johnson, G. Tizazu, G. J. Leggett and G. P. Lopez, *Nanoscale,* 2013, **5**, 3632-3637.

38 P. Shivapooja, L. K. Ista, H. E. Canavan and G. P. Lopez, *Biointerphases,* 2012, **7**, 32.

39 K. Matyjaszewski, H. Dong, W. Jakubowski, J. Pietrasik and A. Kusumo, *Langmuir,* 2007, **23**, 4528-4531.

40 K. N. Plunkett, X. Zhu, J. S. Moore and D. E. Leckband, *Langmuir,* 2006, **22**, 4259-4266.

41 Y. Tang, T. S. Corbitt, A. Parthasarathy, Z. Zhou, K. S. Schanze and D. G. Whitten, *Langmuir,* 2011, **27**, 4956-4962.

42 Q. Yu, Y. Zhang, H. Chen, F. Zhou, Z. Wu, H. Huang and J. L. Brash, *Langmuir,* 2010, **26**, 8582-8588.

43 D. Xia, Z. Ku, S. C. Lee and S. R. Brueck, *Adv. Mater.,* 2011, **23**, 147-179.

44 S. A. Ahmad, G. J. Leggett, A. Hucknall and A. Chilkoti, *Biointerphases,* 2011, **6**, 8-15.

45 D. M. Eby, H. R. Luckarift and G. R. Johnson, *ACS Appl. Mater. Interfaces,* 2009, **1**, 1553-1560.

TOC Graphic

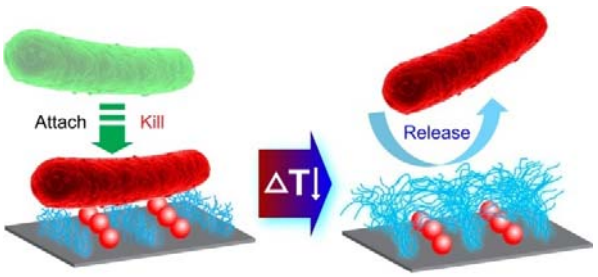

Nanopatterned antimicrobial enzymatic surfaces were developed to control the attachment, killing and release bacteria in response to temperature